Electronic Supplementary Material (ESI) for Physical Chemistry Chemical Physics.

Supplementary Information

High-throughput HSE Study on the Doping Effect in Anatase TiO_2

Jiahua Liu‡, Mouyi Weng‡, Sibai Li, Xin Chen, Jianhang Cen, Jianshu Jie, Weiji Xiao, Jiaxin Zheng* and Feng Pan*

School of Advanced Materials, Peking University, Shenzhen Graduate School, Shenzhen 518055, China.

‡ J. L. and M. W. contributed equally to the present paper.

* Email: zhengjx@pkusz.edu.cn (J. Z.)

* Email: panfeng@pkusz.edu.cn (F. P.)

Band structure information

Computational details for band structures

The computations were also performed by PWmat code, and based on HSE06 functional. Except for the k-point setting, all the other parameters are consistent with what have been described in the "Computational method" in the main text. In this HSE06 non-self-consistent calculation for band structure, the Brillouin zone was sampled by considering a Brillouin Zone Path of Γ—X—M—Γ—Z—R—A—Z consists of the following high symmetry k-points: Γ(0, 0, 0), X(0, 0.5, 0), M(0.5, 0.5, 0), Z(0, 0, 0.5), R(0, 0.5, 0.5), A(0.5, 0.5, 0.5). Between each two high symmetry k-points, five more k-points were inserted, so there are 41 k-points in total.

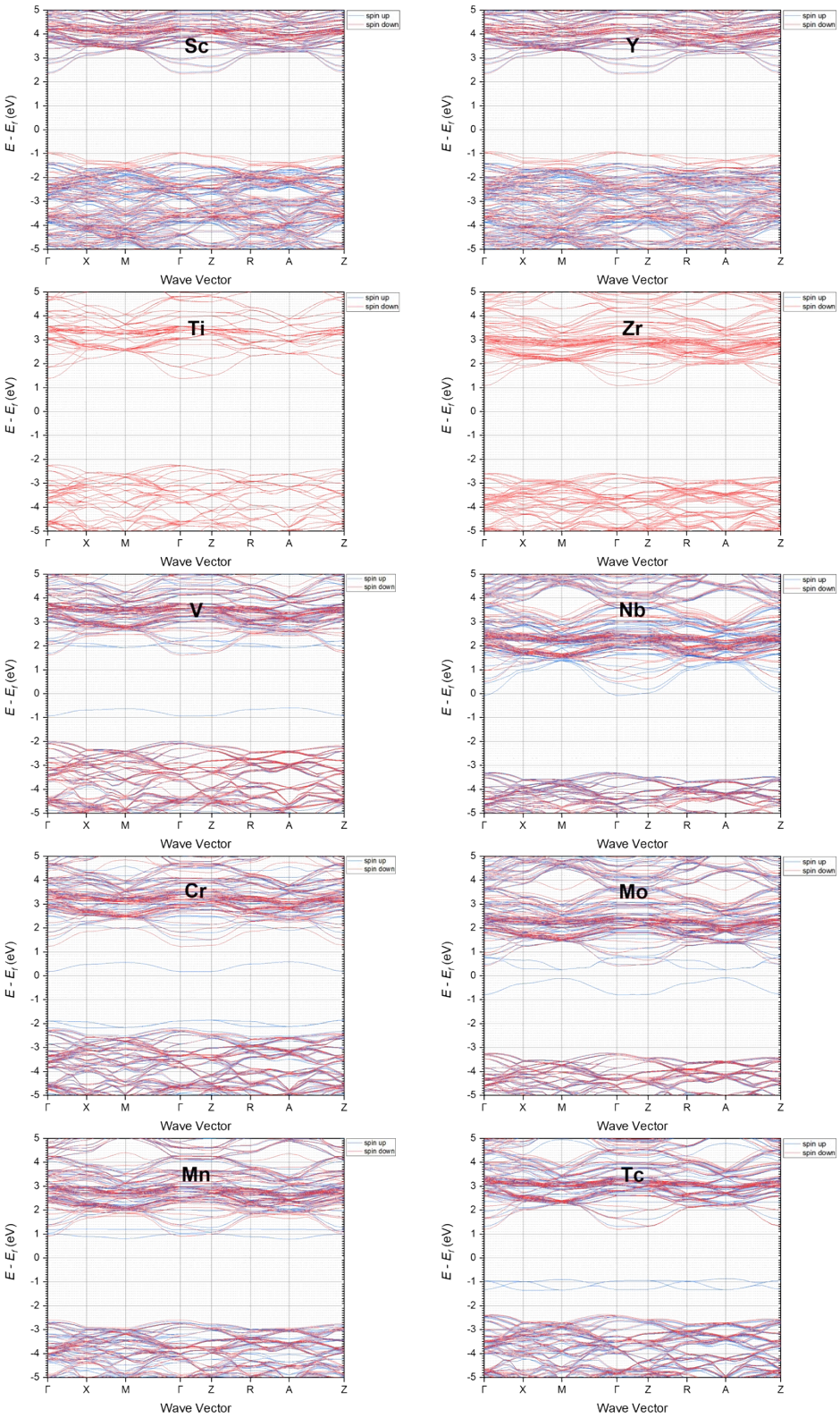

Fig. S1. Band structures of Sc, V, Cr, Mn, Y, Zr, Nb, Mo and Tc-doped TiO_2 systems and pristine TiO_2. The Fermi level is set at zero energy. Different colors donate spin up and spin down.

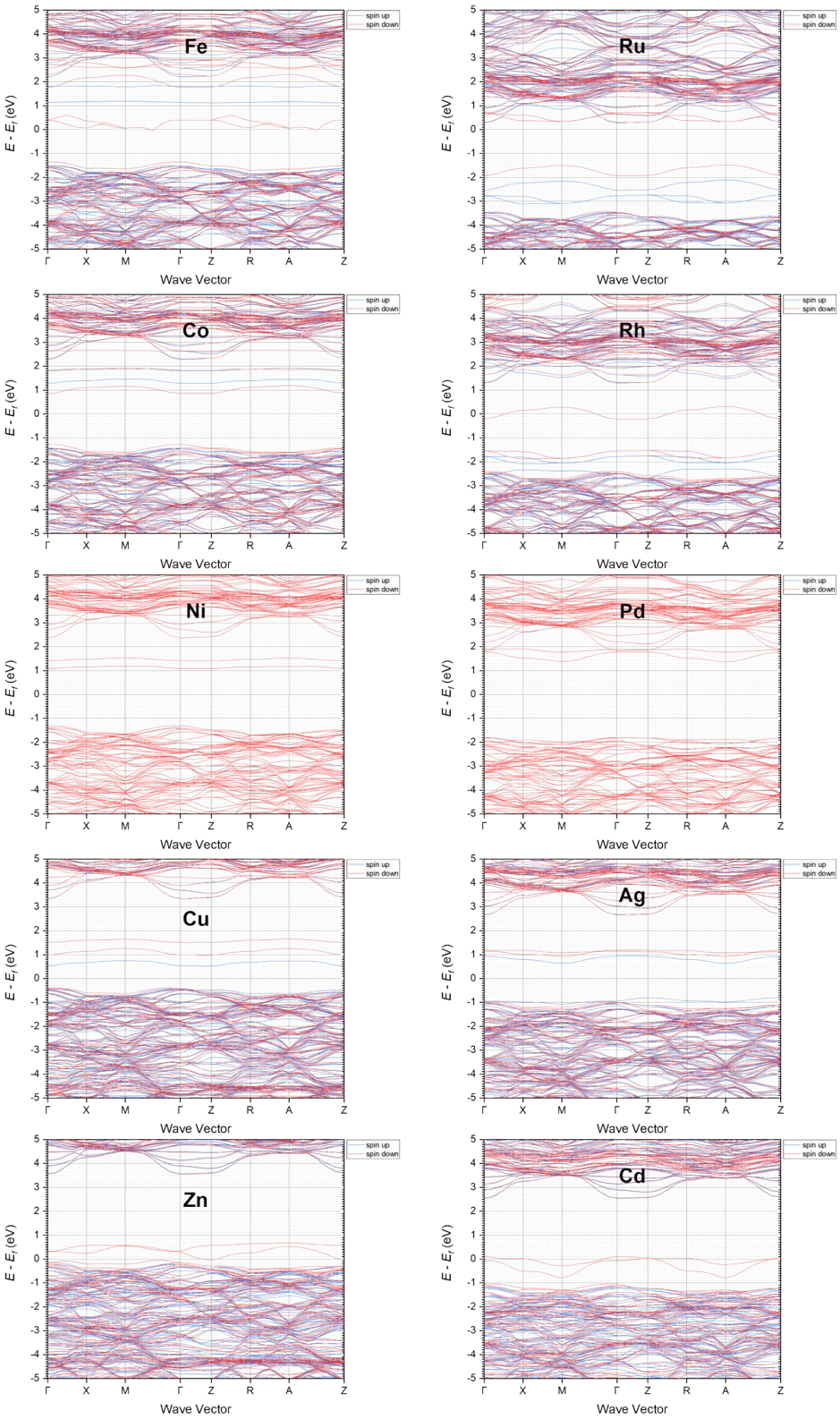

Fig. S2. Band structures of Fe, Co, Ni, Cu Zn, Ru, Rh, Pd, Ag and Cd-doped TiO_2 systems. The Fermi level is set at zero energy. Different colors donate spin up and spin down.

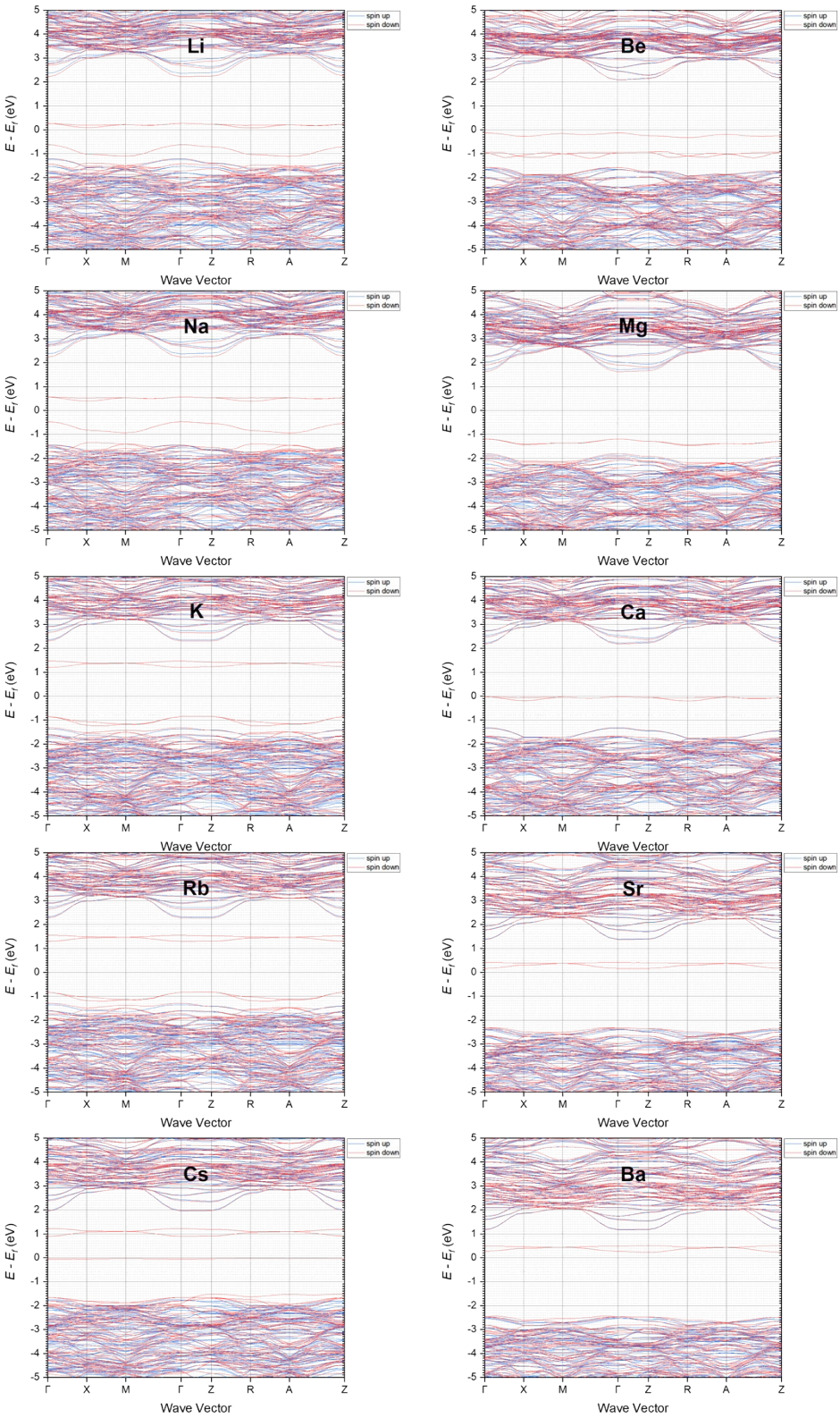

Fig. S3. Band structures of Li, Na, K, Rb, Cs, Be, Mg, Ca, Sr and Ba-doped TiO_2 systems. The Fermi level is set at zero energy. Different colors donate spin up and spin down.

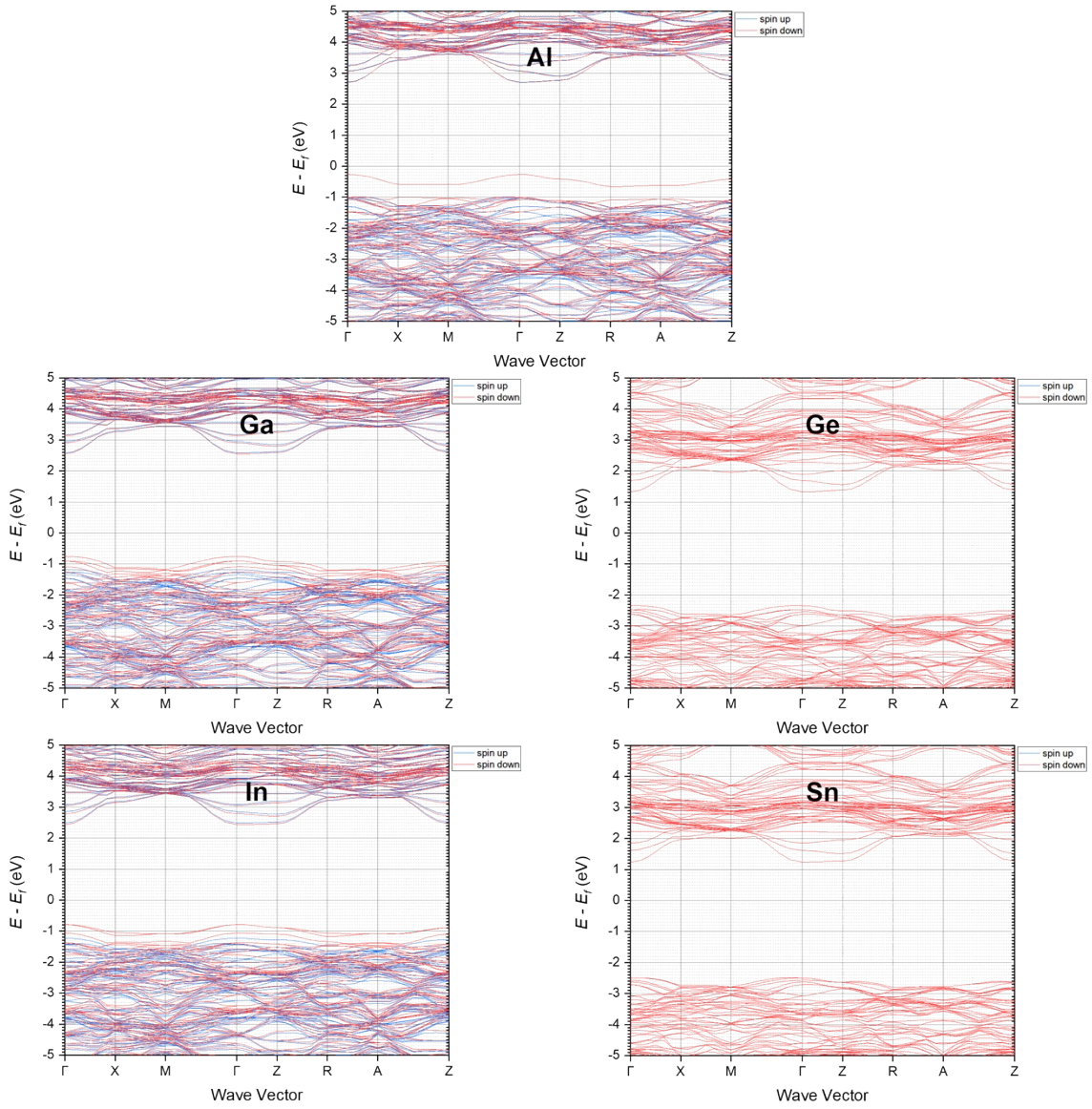

Fig. S4. Band structures of Al, Ga, In, Ge and Sn-doped TiO_2 systems. The Fermi level is at zero energy. Different colors donate spin up and spin down.

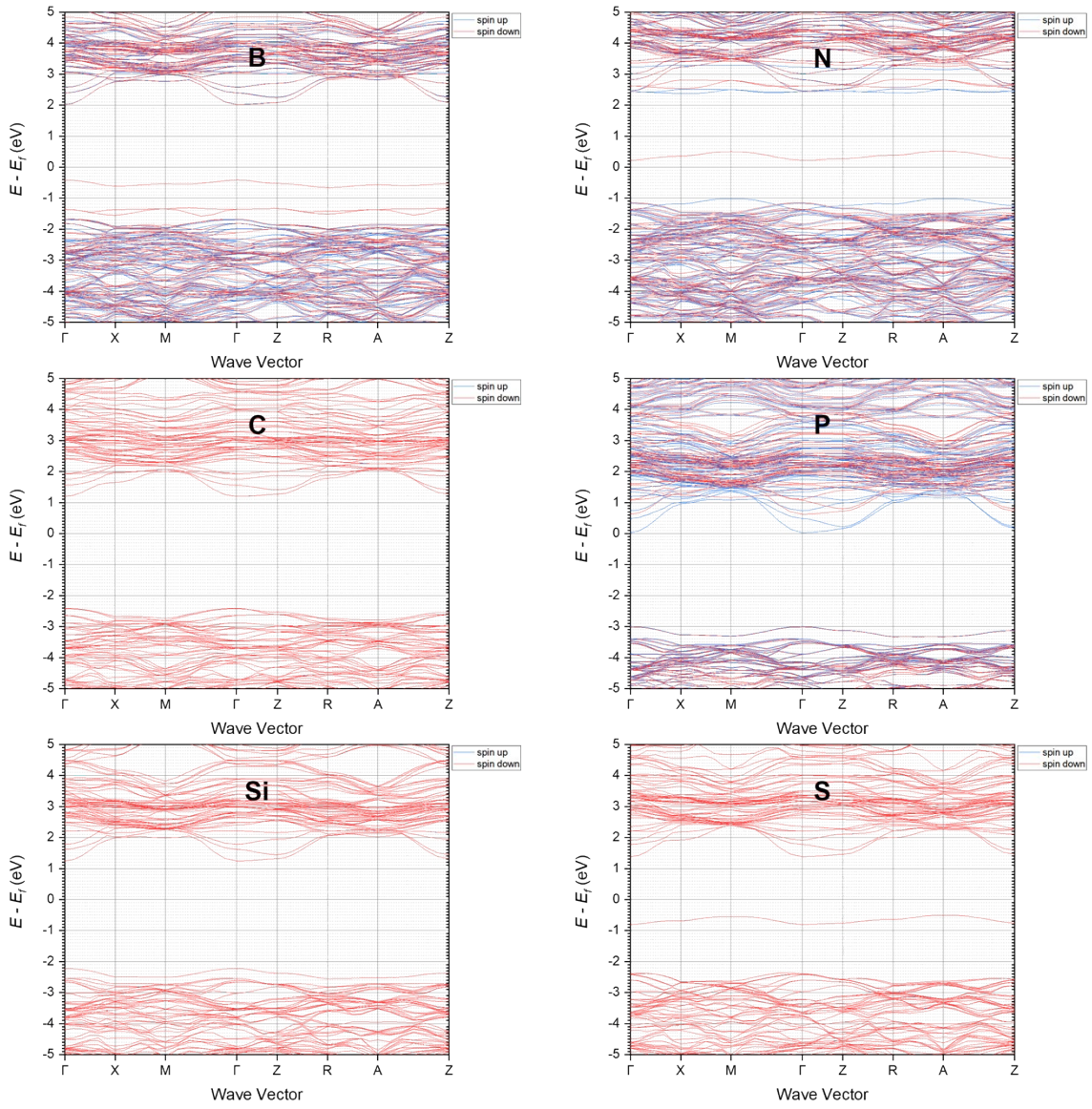

Fig. S5. Band structures of B, C Si, N, P and S-doped TiO_2 systems. The Fermi level is set at zero energy. Different colors donate spin up and spin down.

Table S1. Band information of pristine and doped anatase TiO_2. The calculated band gap values (E_g), the position of conduction band minimum (CBM) and valence band maximum (VBM) described by k-points coordinates (k_{CBM} and k_{VBM}), the distance between the position of CBM and VBM ($|k_{CBM}k_{VBM}|$) and the type of bandgap.

Dopant	E_g(eV)	k_{CBM}	k_{VBM}	$\|k_{CBM}k_{VBM}\|$	Type
TiO_2	3.59	(0, 0, 0)	(0.083, 0.083, 0)	0.12	indirect
Sc	3.18	(0, 0, 0)	(0, 0.083, 0)	0.08	indirect
V	2.20	(0, 0, 0)	(0.5, 0.5, 0.417)	0.82	indirect
Cr	2.03	(0, 0, 0)	(0, 0, 0.5)	0.50	indirect
Mn	3.41	(0.5, 0.5, 0)	(0, 0, 0)	0.71	indirect
Fe	1.33	(0.25, 0.25, 0)	(0, 0, 0)	0.35	indirect
Co	2.14	(0, 0, 0)	(0, 0, 0)	0.00	direct
Ni	2.39	(0, 0, 0)	(0.083, 0.083, 0)	0.12	indirect
Cu	0.91	(0, 0, 0)	(0.083, 0.083, 0)	0.12	indirect
Zn	2.86	(0, 0, 0)	(0.5, 0.5, 0.5)	0.87	indirect
Y	3.25	(0, 0, 0)	(0, 0.083, 0)	0.08	indirect
Zr	3.65	(0, 0, 0)	(0.083, 0.083, 0)	0.12	indirect
Nb	3.23	(0, 0, 0)	(0.083, 0.083, 0)	0.12	indirect
Mo	0.33	(0.5, 0.5, 0.5)	(0.5, 0.5, 0.5)	0.00	direct
Tc	2.06	(0, 0, 0)	(0.5, 0.5, 0.5)	0.87	indirect
Ru	1.77	(0, 0, 0)	(0.5, 0.5, 0.5)	0.87	indirect
Rh	0.97	(0, 0, 0)	(0.5, 0.5, 0.5)	0.87	indirect
Pd	3.18	(0.5, 0.5, 0.5)	(0, 0, 0)	0.87	indirect
Ag	1.44	(0.5, 0.5, 0.5)	(0, 0, 0.5)	0.71	indirect
Cd	2.43	(0, 0, 0)	(0, 0, 0)	0.00	direct
Li	0.70	(0, 0.5, 0.5)	(0, 0, 0)	0.71	indirect
Na	0.85	(0, 0.5, 0.5)	(0, 0, 0)	0.71	indirect
K	2.05	(0, 0, 0)	(0, 0, 0.5)	0.50	indirect
Rb	2.11	(0, 0, 0)	(0, 0, 0.5)	0.50	indirect

Cs	0.92	(0, 0, 0)	(0.1667, 0.5, 0.5)	0.73	indirect
Be	2.21	(0, 0, 0)	(0, 0, 0)	0.00	direct
Mg	2.81	(0, 0, 0)	(0, 0, 0)	0.00	direct
Ca	2.20	(0, 0, 0)	(0, 0, 0)	0.00	direct
Sr	2.47	(0, 0, 0.5)	(0.083, 0.083, 0)	0.51	indirect
Ba	2.66	(0, 0, 0.5)	(0.083, 0.083, 0)	0.51	indirect
Al	2.96	(0, 0, 0)	(0, 0, 0)	0.00	direct
Ga	3.30	(0, 0, 0)	(0, 0, 0)	0.00	direct
In	3.22	(0, 0, 0)	(0, 0, 0)	0.00	direct
Ge	3.67	(0, 0, 0)	(0.083, 0.083, 0)	0.12	indirect
Sn	3.72	(0, 0, 0)	(0.083, 0.083, 0)	0.12	indirect
Si	3.47	(0, 0, 0)	(0, 0, 0)	0.00	direct
C	3.61	(0, 0, 0)	(0, 0, 0)	0.00	direct
B	2.43	(0, 0, 0)	(0, 0, 0)	0.00	direct
N	1.23	(0, 0, 0)	(0.5, 0.5, 0)	0.71	indirect
P	3.04	(0, 0, 0)	(0, 0, 0)	0.00	direct
S	1.89	(0, 0, 0)	(0.417, 0.417, 0.5)	0.77	indirect

Annotation 1: The precise coordinates of the k-points at the specific position of the CBM and VBM depend on the density of the k-points inserted in calculation, so the data of k_{CBM}**,** k_{VBM} and $|k_{CBM}k_{VBM}|$ listed in Table S1 are for reference only. The demonstration of k_{CBM} and k_{VBM} in Table S1 are only for reflecting the type of bandgap, i.e., an indirect gap or a direct gap. Besides, the influence of an indirect bandgap on carriers excitation process can be simply evaluated by referring to the magnitude of $|k_{CBM}k_{VBM}|$. Because the larger the value of $|k_{CBM}k_{VBM}|$, the larger changes of momentum is needed when carriers transition between VBM and CBM occurs.

Annotation 2: In addition, the data of E_g listed in Table S1 are also for reference only. For more detailed energy band information, please refer to the corresponding band diagram displayed above (from Fig. S1 to Fig. S5). Since the doping concentration of 6.25% is already

relatively high, it can be seen from the bandgap diagrams (from Fig. S1 to Fig. S5) that most of the intermediate levels are broadened in different k directions, that is, they have been expanded into intermediate bands. This has a great influence on the process of excitation and transition for the carriers, especially for application scenarios such as photocatalysis, so the intermediate bands (IBs) have been taken into account in determining the values of E_g listed in Table S1. However, we must point out that since the IBs introduced by the doping do not overlap with the intrinsic conduction bands (CBs) or valence bands (VBs) for the most doped systems, the electronic occupancy states that can be accommodated by these isolated IBs are limited. Therefore, for some high current applications, the gap between IBs and the intrinsic VBs or CBs must also be considered, especially for some doped systems where the IBs are far from the intrinsic VBs or CBs. For example, for doping systems such as Mo, Rh, Cs, there is still a large gap between IBs and VBs (2.43, 1.31 and 1.46 eV, respectively); and for Cu, Li, Na-doped systems, there is still a large gap between IBs and CBs (1.68, 1.95 and 1.67 eV, respectively). Hence, despite of the small bandgap obtained by doping these elements, sometimes, the still exiting large gap should also be considered under some circumstances.

We believe that these two annotations can help readers better understand the data listed in Table S1.